



Published in final edited form as:

*J Mol Biol.* 2006 July 14; 360(3): 631–643. doi:10.1016/j.jmb.2006.05.031.

## Structure of a GDP:AlF<sub>4</sub> Complex of the SRP GTPases Ffh and FtsY, and Identification of a Peripheral Nucleotide Interaction Site

Pamela J. Focia\*, Joseph Gawronski-Salerno, John S. Coon V, and Douglas M. Freymann  
Department of Molecular Pharmacology and Biological Chemistry, Feinberg School of Medicine, Northwestern University, 303 E. Chicago Ave., Chicago, IL 60611, USA

### Abstract

The signal recognition particle (SRP) GTPases Ffh and FtsY play a central role in co-translational targeting of proteins, assembling in a GTP-dependent manner to generate the SRP targeting complex at the membrane. A suite of residues in FtsY have been identified that are essential for the hydrolysis of GTP that accompanies disengagement. We have argued previously on structural grounds that this region mediates interactions that serve to activate the complex for disengagement and term it the activation region. We report here the structure of a complex of the SRP GTPases formed in the presence of GDP:AlF<sub>4</sub>. This complex accommodates the putative transition-state analog without undergoing significant change from the structure of the ground-state complex formed in the presence of the GTP analog GMPPCP. However, small shifts that do occur within the shared catalytic chamber may be functionally important. Remarkably, an external nucleotide interaction site was identified at the activation region, revealed by an unexpected contaminating GMP molecule bound adjacent to the catalytic chamber. This site exhibits conserved sequence and structural features that suggest a direct interaction with RNA plays a role in regulating the activity of the SRP targeting complex.

### Keywords

SRP; GTPase; GDP aluminum fluoride; RNA; regulation

### Introduction

The two structurally homologous signal recognition particle (SRP) GTPases Ffh and FtsY play a central role in the assembly of the SRP co-translational protein targeting complex at the membrane.<sup>1,2</sup> Ffh (SRP54) is the component of the SRP ribonucleoprotein that mediates recognition of the hydrophobic signal sequence of the nascent polypeptide. It contains a GTPase subunit that assembles in a symmetric GTP-dependent heterodimer with its structurally homologous GTPase receptor, FtsY (SR $\alpha$ ), to effect the subsequent interaction of the ribosome with the membrane translocon.<sup>3</sup>

Assembly-stimulated GTPase activity of the two SRP GTPases is reminiscent of the behavior of other GTPases in the presence of their GTPase-activating proteins (GAPs).<sup>4</sup> This “reciprocal GAP” activity occurs in the absence of the SRP RNA,<sup>5</sup> but is enhanced in its presence; the system behaves in a way that suggests that the SRP RNA acts catalytically

in the assembly of the complex.<sup>6</sup> The SRP RNA is bound tightly to the M-domain of Ffh,<sup>7</sup> which mediates signal sequence recognition and is linked to the C terminus of the GTPase domain of Ffh.<sup>8</sup> But interactions of the *Escherichia coli* SRP 4.5 S RNA with the Ffh GTPase domain in the free state,<sup>9</sup> and in the neighborhood of the Ffh:FtsY GTPase domain interface in their GTP-assembled complex,<sup>10</sup> have been demonstrated. That the SRP RNA is essential for SRP-mediated targeting, and that *in vitro* it stimulates both the assembly of the heterodimer and subsequent GTP hydrolysis activity of the GTPase targeting complex,<sup>5</sup> raises the possibility that an RNA:protein interaction plays a direct role in the regulation of the SRP GTPase cycle.

The X-ray structure of the heterodimeric complex of the GTPase domains of *Thermus aquaticus* Ffh and FtsY stabilized using the GTP analog GMPPCP<sup>11</sup> in the absence of the SRP RNA<sup>12–14</sup> reveals that they adopt an approximately 2-fold symmetric arrangement that brings their two active sites together to form a shared catalytic chamber at the interface between them. The GMPPCP-stabilized structure represents a “ground state” of the targeting complex, before interaction with other components of the SRP and the conformational rearrangements that deliver the translating ribosome to the membrane translocon. Subsequent structural and biochemical studies support the notion that multiple structural states occur along the path from assembly to disengagement of the targeting complex,<sup>13,15</sup> and that these as yet uncharacterized structural changes may provide points of regulation. Indeed, mutagenesis of *E. coli* FtsY<sup>15</sup> has identified residues at the heterodimer interface that have little effect on assembly but that severely affect the subsequent hydrolysis of GTP by the complex. The question then arises of how the structural behavior of the GTPase complex is regulated during targeting and release of the ribosome nascent chain to the membrane? What interactions allow other components of the SRP targeting machinery to communicate that cargo has been delivered, stimulating GTP hydrolysis and disengaging the targeting complex?<sup>16</sup>

As a first step towards addressing the structural basis for progression from assembly of the Ffh:FtsY heterodimeric complex to activation for nucleotide hydrolysis, we crystallized the complex of the NG domains of the SRP GTPases Ffh and FtsY from *T. aquaticus* in the presence of Mg:GDP:AlF<sub>4</sub>. The GDP:AlF<sub>4</sub> functions as a putative transition-state analog,<sup>17</sup> and has been exploited to determine the structures of other GTPases with their activating proteins, including Ras:RasGAP,<sup>18</sup> Gα:RGS4,<sup>19</sup> and Rho:RhoGAP.<sup>20</sup> In those systems, generally, assembly of the GTPase:activating protein complex is required for binding of the transition-state analog and, conversely, their interaction is stabilized by the transition-state analog relative to ground-state GTP analogs such as GMPPNP and GMPPCP.<sup>21</sup> The coordination number of aluminum is variable, and is somewhat pH-dependent;<sup>22</sup> crystal structures of both AlF<sub>3</sub> and AlF<sub>4</sub><sup>-</sup> nucleotide complexes have been taken as representative of the GTP hydrolysis transition state.<sup>19,23–25</sup>

We find that the SRP GTPase heterodimer complex stabilized by binding GDP:AlF<sub>4</sub> has a structure that is remarkably similar to that of the complex formed in the presence of GMPPCP. The crystal structure reveals that the SRP GTPase heterodimer active site chamber has sufficient plasticity to accommodate two different nucleotide analogs at its interface, and binding of the transition-state analog is accompanied by small shifts of a sequestered water molecule and two arginine side-chains buried within the active site chamber, and small adjustments of two conserved GTPase motifs. In addition, a fortuitous GMP contaminant is found in this structure bound on the surface of the heterodimer adjacent to the FtsY active center. It reveals for the first time an external nucleotide interaction site, comprising several invariant residues from both proteins, that is created at the interface of, and by the formation of, the Ffh:FtsY targeting complex. Its location suggests a role for RNA in the regulation of disengagement of the targeting complex.

## Results

In contrast to other well-characterized GTPase: GAP pairs in the presence of the transition-state analog GDP:AlF<sub>4</sub>, such as Gαi:RGS4,<sup>26</sup> the purified Ffh:FtsY NG domain complex formed in the presence of GDP:AlF<sub>x</sub> is less stable than the complex formed using the ground-state analog GMPPCP (see Experimental Procedures). The binding affinity for *T. aquaticus* Ffh NG and FtsY\_NGd20 measured fluorometrically (Figure 1) was found to be ~10 nM in the presence of the non-hydrolyzable GTP analog GMPPCP, consistent with previous measurements.<sup>5</sup> The binding affinity for assembly of the two GTPases in the presence of GDP:AlF<sub>x</sub>, however, is significantly less, ~2 μM (Figure 1(b)).

The 2.39 Å resolution crystal structure of the GDP:AlF<sub>4</sub>-stabilized complex of the NG GTPase domains of Ffh and FtsY was determined in space group *P*<sub>3</sub><sub>2</sub>, with three copies of the heterodimeric complex in the asymmetric unit. The structures of the three complexes in the crystal are very similar (see Experimental Procedures) and generally the structure of only one complex will be discussed. Throughout the text, residues from FtsY are in italic text, and residues from Ffh are in roman text. The structure has been refined to *R*<sub>cryst</sub> of 0.178 and *R*<sub>free</sub> of 0.252 (Table 1). Two interacting Mg:GDP:AlF<sub>4</sub> groups are bound within the shared active site chamber at the interface between the two proteins. The temperature factors of the active site ligands and water molecules are among the lowest in the structure, consistent with their being tightly coordinated and sequestered from bulk solvent. The AlF<sub>4</sub><sup>-</sup> species is clearly defined by the electron density (Figure 2(a)).

### The GDP:AlF<sub>4</sub> transition-state complex structure is similar to that of the GMPPCP-stabilized state

The structure of the GDP:AlF<sub>4</sub>-stabilized Ffh:FtsY complex (Figure 2(b)) was compared to that of the GMPPCP-stabilized complex (PDB code *1OKK*).<sup>13</sup> The overall structure of the heterodimer is essentially unchanged, with an RMSD over the N and G domains of both Ffh and FtsY of only 0.56 Å over 549 C<sup>α</sup> atoms. Remarkably, the configurations of the ligands in the two structures are nearly identical as well. The two nucleotide analogs interact directly across the heterodimer interface, as in the GMPPCP-stabilized structure, such that the interactions of the fluorine atoms with the 3' OH of GDP across the interface, and with the bound Mg<sup>2+</sup> (Figure 2(c)) echo those seen in the ground-state complex. The relationships of the GDP:AlF<sub>4</sub> ligand relative to the motif I P-loop, the backbone polypeptide of motif III, and the motif II arginine residues *Arg138/Arg142*, which are buried within the chamber and flank the polyphosphate chains, are similar to the earlier structure.<sup>13</sup>

Previously, a superimposition with the Ras:RasGAP:GDP:AlF<sub>3</sub> complex (*1WQI*), suggested to us that the GMPPCP:Ffh:FtsY complex active site chamber would not accommodate the GTP hydrolysis transition state without rearrangement of motif III.<sup>13</sup> However, superimposition on the basis of the ligands in the Ras:RasGAP and GDP:AlF<sub>4</sub>-stabilized Ffh:FtsY complex structure reveals that the motif I P-loops are not superimposable (Figure 3(a)), and the SRP GTPase complex active site chamber exhibits sufficient plasticity to readily accommodate the GDP:AlF<sub>4</sub> without steric clash.

There are a number of well-defined water molecules associated with the nucleotides sequestered within the catalytic chamber; four are in two pairs, reflecting the overall 2-fold symmetry of the complex, and one is not. Each was present in the GMPPCP complex as well and is likely to have relevance to understanding the hydrolysis mechanism of these GTPases. First, a candidate nucleophilic water molecule is evident adjacent to the AlF<sub>4</sub> group in all six active centers within the asymmetric unit (Figure 1(a)), and is positioned by interaction with the carboxylate side-chain of the invariant *Asp135/Asp139* of motif II

(Figure 2(c)). Further, and again echoing the ground-state structure, an “auxiliary water molecule” positioned between the candidate nucleophile and the side-chains of Glu274/*Glu284*, which punctuate the active site at each end,<sup>13,14</sup> bridges the interface of the active site chamber (Figure 2(c)). This auxiliary water molecule occupies a position, with respect to the nucleophilic water molecule, similar to that of the side-chain carbonyl oxygen atom of invariant Gln61 in Ras (Figure 3(a)).<sup>18,27</sup> Its juxtaposition to the invariant residues Glu274/*Glu284*, suggests that it may contribute to activation of the nucleophilic water molecule.

Finally, there is a “central water molecule” sequestered completely within the active site chamber, that is located between the two nucleotides and the two invariant arginine side-chains that flank them (Figures 2(c) and 3(b)). This water molecule has no partner, and so is asymmetric, and it moves relative to its position in the structure of the GMPPCP complex.<sup>13</sup> Asymmetry of two buried invariant arginine side-chains (*Arg138/Arg142*) within the otherwise very symmetric GMPPCP: Ffh:FtsY complex was noted previously.<sup>13</sup> In the GDP:AlF<sub>4</sub> structure, this asymmetry is amplified at the center of the active site chamber (Figure 3(b)), as the central water molecule shifts by over 1 Å in the direction of the phosphate groups of the FtsY nucleotide. It no longer makes contact with the Ffh nucleotide or the *Arg142* side-chain. This shift of the central water molecule is the largest that occurs within the G domains of the two proteins between the GMPPCP and GDP:AlF<sub>4</sub>-bound states.

The new configuration of the central water molecule, and its interactions with Arg138, which itself loses a hydrogen bond to the Ffh  $\gamma$ -phosphate group and forms a new hydrogen bond to *Arg142*, is consistent with its playing a role in stabilizing the developing negative charge during GTP hydrolysis. The central water now bridges what would correspond to the scissile bond in GTP, hydrogen bonding to the AlF<sub>4</sub> F1 and the O3B of the FtsY GDP, as well as to O2A. FtsY *Arg142* forms an additional interaction with the FtsY AlF<sub>4</sub>, which corresponds to the leaving group, and could act as a hydrogen bond donor. Two invariant glutamine residues, Gln144/*Gln148*, positioned by hydrogen bonds to a magnesium-coordinated water molecule and the  $\alpha$ -phosphate group of each nucleotide (Figure 3(b)), provide a scaffold for stabilizing the positions of Arg138/*Arg142*, and thus the central water molecule, with respect to the phosphate groups of the GTP molecules. Thus, the more extended conformation of Arg138 is stabilized by a water-mediated interaction *via* NE to the motif II backbone and through this same water molecule with Gln144 OE1, while the bent configuration of *Arg142* (towards its own nucleotide) is stabilized by a direct hydrogen bond with NE to the motif II backbone and interaction with *Gln148* OE1 *via* NH2.

### **GMP is bound on the surface of the GTPase heterodimer at a common nucleotide-binding motif**

An unexpected electron density feature external to the active site chamber on one side of the heterodimer complex exhibited a large flat region suggestive of a purine base, and a strong peak consistent with one, but not two, 5' phosphate groups (Figure 4(a)). We subsequently determined that the GDP used in crystallization was substantially degraded, and assign the feature as a molecule of GMP. It is bound at a crystal lattice contact that is present for each of the three heterodimers in the asymmetric unit; however, its presence is not necessary for the crystals to form. The interactions of the bound GMP are extensive, and well defined, the purine ring, ribose hydroxyl group and the 5' phosphate group are each contacted by a set of conserved residues assembled at the complex interface (described below). Its interactions across the crystal contact, also *via* the 5' phosphate group, are non-specific, with two hydrogen bonds, one water-mediated, to a serine residue in a neighboring complex.

The GMP molecule is bound in a pocket defined by motifs II and III of FtsY and the invariant Glu274 of the “closing loop” of Ffh,<sup>28</sup> and so is surrounded by and interacts with

highly conserved residues from both proteins (Figure 4(b)). The side-chain of invariant Ffh Glu274 provides two hydrogen bonds, one direct (OE2 to N1 of the purine ring), the other water-mediated (main chain nitrogen atom to GMP O6). The adjacent conserved Lys275 interacts with the 5' phosphate group in two of three complexes in the asymmetric unit. The side-chain of invariant *Glu205*, located along the  $\alpha 2$  helix following motif III, forms a hydrogen bond to the GMP 2' OH. And, at the center of the pocket, the carbonyl oxygen atom of invariant FtsY motif III *Gly194* hydrogen bonds to the GMP 2-amino group (and to the auxiliary water molecule, see below). This interaction, in particular, by exploiting the 2-amino hydrogen bond donor, provides apparent specificity for interaction with a guanine base. Finally, the purine ring is sandwiched by hydrophobic interactions, the conserved residue *Phe141*, of motif II (sequence *DTFRAGA*<sup>29</sup>), provides  $\pi$ - $\pi$  stacking interactions on one face, and invariant *Leu202*, located along helix  $\alpha 2$ , packs against the other face. Other conserved residues contribute to the architecture of the binding site; in particular, invariant motif III residue *Arg195* hydrogen bonds *via* NH1 to the carbonyl group of *Leu202* and to the *Glu205* side-chain OE2, and is itself held in place by an interaction *via* NH2 to the carbonyl group of *Ala193* (Figure 4(b)). The latter interaction contributes to the external nucleotide-binding site by stabilizing the backbone conformation of FtsY motif III. *Arg195* is one of the residues in *E. coli* FtsY that, when mutated in the context of the SRP:FtsY targeting complex, affects specifically the GTP hydrolysis step (Figure 5).

The residues that define the structure of the external GMP binding site, the hydrophobic pocket between *Phe141* and *Leu202*, the carboxylate interaction provided by *Glu205*, and the hydrogen bond of the *Gly194* carbonyl oxygen atom, are invariant in the sequences of prokaryotic FtsY. Such interactions are common to nucleotide-binding proteins; anionic interaction with a nucleotide hydroxyl group,<sup>30–32</sup> and aromatic stacking against a nucleotide base occur in the DNA repair enzymes,<sup>33,34</sup>  $\gamma$ -tubulin,<sup>35</sup> the U1A spliceosomal protein,<sup>36</sup> the purine and pyrimidine phosphoribosyltransferases<sup>32,37</sup> and aspartyl-tRNA synthetase.<sup>38</sup> Indeed, the binding configuration at the SRP GTPase external nucleotide site is specifically reminiscent of similar arrangements in crystal structures of the editing complex of Klenow fragment<sup>34,39</sup> and AMP-bound adenine phosphoribosyltransferase (APRT)<sup>40</sup> (Figure 6). In the 3' to 5' exonuclease active site of the Klenow fragment, the 3'-terminal base of the single-stranded DNA is positioned between Leu361 and Phe473, and the 2'-OH interacts with Glu357 (Figure 6(b)). A similar arrangement was observed in an earlier structure co-crystallized with a single nucleotide bound.<sup>33</sup> In APRT (as in other purine and pyrimidine phosphoribosyltransferases), the base of the nucleoside monophosphate reaction product is sandwiched between an aromatic residue providing  $\pi$ - $\pi$  stacking on one face and a leucine (or isoleucine) residue on the other, with a hydroxyl group coordinated via a carboxylate side-chain (Figure 6(c)).<sup>32,40</sup> In all three systems, the residues that contribute to these sites are highly conserved; however, their sequence contexts are distinct. Thus, in APRT, the Glu/Leu pair are neighbors in the highly conserved PRT signature motif,<sup>41</sup> while the aromatic residue (here Phe26) is from a separate domain.

### The external GMP site juxtaposes the FtsY active center and an SRP RNA interaction surface

The highly conserved surface-exposed residues that contribute to the GMP binding site are coupled to catalytic elements within the active site chamber of the heterodimer. Thus, FtsY motif II residue *Phe141*, which packs against the GMP base (Figure 4(b)) is adjacent to motif II residue *Arg142*, part of the asymmetric arginine pair buried within the active site chamber that flanks the phosphate groups of the two active site nucleotides (Figures 2(c), 3(b)). Even more direct is the hydrogen bonding interaction of FtsY motif III residue *Gly194* with the 2-amino group of GMP. This glycine is universally conserved in GTPases, and its backbone orientation plays a direct role in the mechanism of GTP hydrolysis.<sup>42</sup> Residues

*Leu202*, which contributes the opposite face of the purine base binding pocket, and *Glu205*, which hydrogen bonds to the GMP hydroxyl group (Figure 4(b)), occur along helix  $\alpha 2$  adjacent to FtsY motif III, corresponding to the “switch 2” region that is conformationally coupled to interactions at the GTPase active center in other GTPases.<sup>43</sup> Invariant Glu274 that extends from the “closing loop” of Ffh provides two interactions with the GMP, at N1 and O6, and, via the auxiliary water molecule, an interaction with the nucleophilic water molecule at the FtsY nucleotide (Figure 4(b)). The auxiliary water molecule also bridges interactions of both Glu274 and the FtsY nucleophilic water molecule to the carbonyl group of the invariant FtsY motif III residue *Gly194*. Because Glu274 interacts also with the nucleotide from its own subunit (OE1 to O2' OH) (Figures 2(c) and 4(b)), an externally bound GMP nucleotide is therefore in position to interact indirectly with both nucleotides within the catalytic chamber.

In the assembled Ffh:FtsY heterodimer there are two regions of highly conserved sequence that are exposed on its lateral face and that can be distinguished from residues that contribute to the interface itself (compare Figure 7(a) and (b)). The first is defined primarily by invariant Glu274 of the closing loop of Ffh and residues of FtsY motifs II and III, and helix  $\alpha 2$ , and includes the external GMP-binding site, generating what we term the activation region of the heterodimer interface. The second occurs near the interface of the N and G domains of Ffh. A patch of highly conserved residues at the junction of the C terminus of Ffh (which would link to its C-terminal M domain) and its N/G interface (Figure 7(b)) includes the conserved ALLEADV loop of the Ffh N domain between  $\alpha N2$  and  $\alpha N3$ , and generates a cationic surface comprising residues from both the C terminus and the DARGG motif that follows motif IV.<sup>28</sup> Together they provide a somewhat contiguous path comprised of charged and polar residues that extends from the external nucleotide site towards the N domains of Ffh and FtsY.

The conserved surface corresponds almost exactly to the surface against which the SRP RNA must pack, as mapped by a recent site-directed RNA cleavage study of the assembled *E. coli* Ffh:FtsY:4.5S RNA complex.<sup>10</sup> The 4.5 S RNA interaction extends across the Ffh:FtsY heterodimer along one face (the “front”) that extends from the activation region defined here towards the second conserved patch at the Ffh N/G interface and the N domains of the two proteins.<sup>10</sup> The most highly conserved region of the SRP RNA, the motif IV hairpin,<sup>44</sup> can be located to the neighborhood of the activation region, and there are three sites, one in Ffh and two in FtsY, at which cleavage near the 4.5 S RNA hairpin tetraloop in the assembled SRP:FtsY complex can be mapped. These residues, corresponding to Ffh Glu150 and FtsY *Thr167* and *His200*,<sup>10</sup> outline the activation region and bracket the external nucleotide-binding site (yellow spheres in Figures 2(b) and 7(b)).

## Discussion

The binding affinity for assembly of the two GTPases in the presence of GDP:AlF<sub>x</sub>, ~3  $\mu$ M, is almost 300-fold lower than for the GMPPCP complex and it is not surprising, therefore, that the structure reported here does not define a GTP hydrolysis transition-state conformation of the protein complex, and does not differ remarkably from the GMPPCP-stabilized structure. It suggests, instead, that the heterodimer has sufficient plasticity to assemble in the presence of a non-native nucleotide analog pair. And it prompts several possible explanations for this behavior. First, the transition-state analog bound in this structure may be a sufficiently poor mimic of the expected trigonal-planar penta-coordinate GTP hydrolysis transition state that its binding does not reveal an activated conformation of the proteins. Alternatively, the catalytic state of the complex may not accommodate binding of a symmetric transition-state species, instead requiring alternate configurations, in effect reflecting a sequential hydrolysis mechanism. Finally, the structure of the heterodimeric

complex may not be stabilized for activation of the GTP hydrolysis transition state in the absence of additional interactions with other components of the targeting machinery (e.g. 4.5 S RNA, ribosome, translocon).

Nevertheless, the changes that are observed, in particular movement of the central water molecule and the re-configuration of two buried arginine side-chains, provide some insight into the conformational freedom within the active site chamber of the SRP GTPase heterodimer (Figure 3). They are suggestive, in addition, of an alternating hydrolysis mechanism,<sup>4,13</sup> as a simple reversal of configuration would shift the central water molecule closer to the Ffh-bound nucleotide to interact with *Arg142* in its more extended conformation, with *Arg138* bent toward the Ffh nucleotide phosphate chain. We propose, therefore, that the two pairs of invariant residues Arg/Gln internal to the catalytic chamber in each protein may couple to provide a variable conformational scaffold for stabilizing the position of the central water molecule and active site arginine residues with respect to the phosphate groups of the bound GTP molecules.

The observation of a nucleotide-binding site defined by a conserved sequence and characteristic structural arrangement external to the catalytic chamber at the surface of the assembled SRP GTPase heterodimer in the vicinity of the active center of FtsY (but not Ffh) was unexpected. That it constitutes a functionally significant activation region that can play a role in regulating GTP hydrolysis, and, therefore, disassembly of the SRP targeting complex, is supported by several lines of evidence. First, highly conserved residues of the FtsY GTPase sequence motifs II and III are associated with the site, and several residues of those motifs are directed towards the external activation region rather than the active center.<sup>13</sup> The functional significance of these conserved residues of motifs II and III was previously unknown. Second, the structural arrangement that defines the interactions of the activation region is characteristic of nucleotide-binding pockets observed in other such proteins (Figure 6). These provide a well-defined and extensive set of van der Waals, hydrogen bonding, and ionic interactions that position a fortuitously present GMP molecule precisely at that interface (Figure 4). Third, mutations of some of these residues (e.g. FtsY *Arg195*) (Figure 5) affect the rate of GTP hydrolysis in the assembled complex but have little effect on assembly itself<sup>15</sup>. They therefore must play some role in catalysis, but are directed away from the active center and poised instead, perhaps, for interaction with external factors (Figure 4(b)). Fourth, an extensive region of highly conserved sequence extends across the surface of the complex, forming two patches that span the GMP-binding site at the activation region and the N/G domain interface along one face of the complex (Figure 7(b)). Finally, the 4.5 S RNA interaction surface defined by site-directed footprinting studies<sup>10</sup> includes the activation region, and the tetraloop sequence of the conserved motif IV of the RNA, demonstrated to affect GTPase activation,<sup>10</sup> is placed, in this model, adjacent to the external GMP nucleotide-binding site.

Biochemical studies of the effects of SRP RNA on various components and on the formation and behavior of the Ffh:FtsY targeting complex have shown that SRP RNA, when bound to Ffh, enhances the association and GTPase activity of Ffh and FtsY,<sup>45</sup> and increases dramatically the rate at which GTP-loaded SRP and SR associate and dissociate.<sup>5</sup> The proximity of an external nucleotide-binding pocket to the active center of FtsY and to both nucleotides within the shared catalytic chamber suggests the existence of a direct regulatory interaction between SRP RNA and the active center of the heterodimeric GTPase. This interaction may be mediated by FtsY residue *Gly294* and the side-chain of Ffh *Glu274*, which couple the external site to the active site chamber (Figure 4(b)). We infer from the binding of a guanine nucleotide to the external site that any interaction between the 4.5 S RNA and the Ffh:FtsY NG heterodimer at that site requires that a nucleotide base be flipped out. Such configurations are relatively common, as, for example, in structures of the

conserved motif IV of the 4.5 S RNA alone,<sup>46</sup> the SRP RNA complex with Ffh M domain,<sup>47</sup> the RNA complexes of the SRP Alu domain,<sup>48</sup> and DNA-editing complexes involved in repair and excision of 8-oxoguanine:adenine mispairs.<sup>49,50</sup>

Previously, mutations of residues associated with the activation region, in particular *Arg195*, have been assayed in the context of the assembled SRP: FtsY complex<sup>15</sup> and found to exhibit deficiencies in GTPase activation. It is possible that these defects, rather than reflecting a contribution to the chemistry of GTP hydrolysis *per se* (as in an arginine finger mechanism<sup>51</sup>), reflect instead interactions of the activation region with the 4.5 S RNA of the SRP. In this scenario, at the appropriate moment in the targeting cycle, the RNA then plays a direct role, yet to be discovered, in activating GTP hydrolysis by the Ffh:FtsY GTPase heterodimer.

## Experimental Procedures

### Purification of Ffh and FtsY NG domain constructs

The NG domain of *T. aquaticus* Ffh was expressed and purified as described.<sup>12</sup> A vector, pJGS3, expressing the protein FtsY\_NGd20 in which the N-terminal 20 residues of *T. aquaticus* FtsY are deleted, was constructed by PCR mutagenesis of pTP88<sup>12</sup> using the QuikChange II Site-Directed Mutagenesis Kit (Stratagene). Constructs were verified by sequencing at the Northwestern University Biotechnology Laboratory. Protein was expressed from pJGS3 using the *E. coli* Rosetta-2(DE3)/pLysS strain (Novagen). FtsY\_NGd20 was purified from heat-treated cell lysates<sup>11</sup> by elution from a 5 ml HiTrap Blue column using a linear gradient of 0–1.0 M NaCl, desalting on a HiPrep 26/10 desalting column, and elution from a 5 ml HiTrap SP column equilibrated with 10 mM Hepes (pH 7.5), 1.0 mM DTT, using a linear gradient of 0–1.0 M NaCl. The SP fraction was desalted again, and then passed over a 5 ml HiTrap Q Sepharose HP column equilibrated with 50 mM Tris-HCl (pH 8.0), 1.0 mM DTT, and eluted using a linear gradient of 0–1.0 M NaCl. The protein was >95% pure as evaluated by SDS-PAGE and stored at –20 °C.

For fluorometric studies a cysteine residue was introduced along helix  $\alpha_3$  at position 235 in *T. aquaticus* Ffh and the construct expressed and purified as for the native protein. Protein was prepared for labeling by reducing in the presence of 1 mM Tris[2-carboxyethyl]phosphine and 50 mM Tris-HCl (pH 8.0) at room temperature, followed by buffer exchange into 50 mM Hepes (pH 7.5). The protein, at 50  $\mu$ M in the same buffer, was labeled by addition of 1 mM 5-(((2-iodoacetyl)amino)ethyl)amino naphthalene-1-sulfonic acid (IAEDANS) and incubation at room temperature for 2 h. The reaction was desalted to remove unconjugated fluorophore, and subsequently purified by anion-exchange HPLC over a 5.0 ml QSepharose HP column (Amersham-Pharmacia) in 50 mM Tris-HCl (pH 8.0) buffer, eluted using a gradient of 0–1.0 M NaCl. Labeling was confirmed to be >99% by measurement of absorbance at 280 nm/336 nm (protein/fluorophore  $\lambda_{\text{abs}}$ ) and by dithionitrobenzoic acid quantification of free cysteine.

### Formation and characterization of the GDP:AlF<sub>4</sub>-bound complex

Preliminary experiments to assay for the GDP:AlF<sub>x</sub>-stabilized complex were carried out with 15  $\mu$ M Ffh NG and 10  $\mu$ M FtsY\_NGd20 in 50 mM Hepes (pH 7.5), 2 mM MgCl<sub>2</sub>, 50 mM NaCl in the presence of 2 mM AlCl<sub>3</sub>, 20 mM NaF, and 1 mM GDP.<sup>18</sup> After incubation at 37 °C for 20 min, complex formation was assayed by gel-filtration chromatography using a Superdex 75 HR 10/30 gel-filtration column equilibrated with 50 mM Tris-HCl (pH 8.0), 2 mM MgCl<sub>2</sub>, 50 mM NaCl. Formation of the FtsY\_NGd20/Ffh NG domain complex occurred rapidly and the complex peak could be purified readily by gel-filtration chromatography. However, in contrast to the behavior with the GTP analog GMPPCP,<sup>12</sup>



complex formation did not go to completion and, on incubation of the purified, diluted, complex sample at room temperature, appreciable dissociation occurred (to ~33% after 2 h, as measured by the  $A_{280}$  peak heights for the monomeric and heterodimeric species). Because the  $K_D$  for the GDP:AlF<sub>x</sub>-stabilized complex was substantially higher than that for the GMPPCP-stabilized complex, crystallization screens were set up without prior purification. By maintaining the concentrations of the two proteins at >250  $\mu$ M (for Ffh) and >200  $\mu$ M (for FtsY), the fraction of complex species was estimated to remain >80% under the assay conditions. Preparation of the GDP:AlF<sub>4</sub>-stabilized complex for crystallization was carried out using 250  $\mu$ M Ffh NG M294 and 200  $\mu$ M FtsY\_NGd20 in 50 mM Hepes (pH 7.5), 2 mM MgCl<sub>2</sub>, 50 mM NaCl, 2 mM AlCl<sub>3</sub>, 20 mM NaF.<sup>18</sup> GDP was added to a final concentration of 1 mM, and 440  $\mu$ l reactions were incubated with shaking at 37 °C for 1 h before setting up the crystallization trials.

### Crystallization and data collection

A diffraction-quality crystal form was obtained by the sitting-drop, vapor-diffusion method directly from an initial robotic crystallization screen using 1  $\mu$ l of GDP:AlF<sub>4</sub> complex plus 1  $\mu$ l of reservoir solution at room temperature. A single crystal was harvested from 0.1 M Tris-HCl (pH 8.5), 25% (w/v) PEG 8000 (Nextal PEGS #46) mother liquor by extensive dissection of a highly clustered group and transferred to a cryoprotectant solution supplemented with 10% (v/v) ethylene glycol. Although the crystal cracked on addition of the cryo-protectant solution, intact shards were mounted quickly in a nylon loop and flash-cooled in liquid nitrogen. Data were measured at APS sector 32 on a 165 cm MarCCD, using a wavelength of 0.97625 Å, a detector distance of 150 mm, an oscillation angle of 0.5°. The exposure time was 5 s with an unattenuated beam (BL 32-ID-B). Data were reduced using MOSFLM<sup>52</sup> and SCALA,<sup>53</sup> yielding 99.6% complete data to 2.39 Å resolution with an overall  $R_{\text{sym}}$  of 0.101 (Table 1).

### Structure solution and refinement

The structure was determined using molecular replacement with PHASER.<sup>54</sup> The search model was a GMPPCP-stabilized heterodimer (*IOKK*),<sup>13</sup> with ligands and water molecules removed. A solution of three heterodimeric complexes in the asymmetric unit was found (LLG = 6626). Following initial crystallographic refinement in REFMAC,<sup>55</sup> an initial  $F_o-F_c$  electron density map clearly revealed the bound ligands. Solvent structure was built using ARP/wARP,<sup>56</sup> and the ligands placed and the structure built using O.<sup>57</sup> The initial  $F_o-F_c$  maps clearly indicated the bound Mg<sup>2+</sup>GDP group, and indicated that the bound AlF<sub>x</sub> species was AlF<sub>4</sub><sup>-</sup>, not AlF<sub>3</sub>, as the 2.39 Å resolution electron density map clearly indicated the square planar geometry (Figure 2(a)). The model consists of three Ffh chains (residues 4–293), three FtsY chains (residues 21, 23, 26–303), six bound Mg<sup>2+</sup> GDP:AlF<sub>4</sub><sup>-</sup> ligands, three external site GMP molecules and 621 solvent molecules. The refinement statistics are summarized in Table 1. The 7.5% difference between  $R_{\text{cryst}}$  and  $R_{\text{free}}$  is likely due to relatively poor diffraction, as reflected in the high overall  $R_{\text{sym}}$ . NCS restraints were not used during refinement. The three complexes are superimposable with an RMSD over Ca atoms of 0.46 Å and 0.63 Å, respectively, for Ffh (290 Ca atoms) and FtsY (276 Ca atoms), between complexes 1 and 2 (chains A/D and B/E), 0.65 Å and 0.68 Å between complexes 1 and 3 (A/D and C/F), and 0.65 Å and 0.56 Å between complexes 2 and 3 (B/E and C/F). These values reflect the relative motion of the N and G domains within each protein pair;<sup>58</sup> for example, when the superimposition is limited to the G domains only, for the first pair (A/D, B/E, above) the RMSD values decrease to 0.17 Å and 0.18 Å for Ffh (182 Ca atoms) and FtsY (188 Ca atoms). The overall RMSD on Ca atoms relative to the GMPPCP-stabilized complex structure (*IOKK*) is ~0.56 Å; for each component of the heterodimer, Ffh and FtsY, superimposed separately, the RMSD is ~0.45 Å. The largest shifts between the G domains

of the Mg:GMPPCP and Mg:GDP:AlF<sub>4</sub> structures occur at motif I and III residues Gly108/*Gly112* and Gly190/*Gly194*, which shift ~0.7 Å and ~0.6 Å, respectively. Models were superimposed using LSQMAN.<sup>59</sup>

### Fluorescence binding measurements

Fluorometric assembly assays were carried out in the presence 50 mM Hepes (pH 7.5), 50 mM NaCl, 2 mM MgCl<sub>2</sub>, 0.5 μM nucleotide (GMPPCP, or GDP). The GDP-AlF<sub>4</sub> complex assembly titrations included 0.5 mM Al (NO<sub>3</sub>)<sub>3</sub> and 20 mM NaF. FtsY\_NGd20 was titrated against 0.5 μM IAEDANS-labeled Ffh NG as a 1:2 dilution series. The assays were incubated for 30 min at 37 °C followed by centrifugation at 1000 g for 5 min prior to measurement. Assembly was measured by fluorescence resonance energy transfer (FRET) using a Tecan Safire2 spectrofluorometer ( $\lambda_{\text{ex}} = 285 \text{ nm}$  (20 nm bandwidth),  $\lambda_{\text{em}} = 550 \text{ nm}$  (10 nm bandwidth)). The assay exploits the presence of three tryptophan residues in FtsY, each located ~30–35 Å from the fluorophore in the heterodimeric complex, that together yield a 2.5-fold increase in IAEDANS emission intensity from labeled Ffh upon formation of its complex with FtsY. Data were analyzed using Prism 4 (GraphPad) following subtraction for background, and the fractional difference intensity  $\gamma = (I_{\text{obs}} - I_{\text{free}}) / I_{\text{free}}$  was fit by non-linear regression using the binding equation:

$$\gamma = (Q - 1) \left[ (X + \text{Ligand}_{\text{tot}} + K_D) - \left( (X + \text{Ligand}_{\text{tot}} + K_D)^2 - 4X\text{Ligand}_{\text{tot}} \right)^{1/2} \right] / (2\text{Ligand}_{\text{tot}})$$

where Q is the ratio of the fluorescence intensity of the bound and free probe (IAEDANS-Ffh NG) and  $X = [\text{FtsY\_NGd20}]$  in the titration.

### Sequence analysis

The amino acid sequences of prokaryotic Ffh (52 sequences) and FtsY (23 sequences) were obtained from the SRPDB,<sup>60</sup> and the sequence alignments were inspected and corrected by hand using INDONESIA (D. Madsen *et al.*, unpublished results). This program then generated a sequence entropy, defined as  $S(m_i) = -\sum c_{ia} \log p_{ia}$  (where  $c_{ia}$  is the count of amino acid residue  $a$  at position  $i$ , and  $p_{ia}$  is the probability of amino acid residue  $a$  at position  $i$ ), at each position in the alignment that was mapped to the  $B$ -factor column in the coordinate file to be plotted onto the molecular surface using GRASP<sup>†</sup>.

### Protein Data Bank accession number

Coordinates and structure factors have been submitted to the PDB with accession numbers 2cnw and r2nwsf.

### Acknowledgments

We thank Kristin A. Dietrich and Amanda C. Drennan for assistance with the construction and purification of the cysteine mutant of the Ffh NG domain. We thank Robert J. Keenan for critical comments on the manuscript. This work was supported by grant GM058500 from the NIH, and by support from the R.H. Lurie Comprehensive Cancer Center to the Structural Biology Facility at Northwestern University. Portions of this work were carried out at several Advance Photon Source beamlines (COM-CAT Sector 32, BioCARS Sector 14, SBC Sector 19). Use of the Argonne National Laboratory beamlines at the Advanced Photon Source was supported by the U.S. Department of Energy, Office of Energy Research, under contract W-31-109-ENG-38. Use of the BioCARS Sector 14 was supported by the NIH, National Center for Research Resources, grant number RR07707.

P.J.F. carried out the crystallographic work, structure refinement and interpretation; J.G.S. was responsible for mutagenesis, crystallization and FRET studies; J.S.C.V and J.G.S. purified and characterized assembly of the

<sup>†</sup><http://www.trantor.bioc.columbia.edu/grasp/>

protein complex; D.M.F. contributed to the structure solution and model building; P.J.F and D.M.F wrote the manuscript.

## Abbreviations used

<b>SRP</b>	signal recognition particle
<b>GAP</b>	GTPase-activating protein
<b>1,5-IAEDANS</b>	5-(((2-iodoacetyl)amino)ethyl)amino)naphthalene-1-sulfonic acid
<b>FRET</b>	fluorescence resonance energy transfer

## References

- Keenan RJ, Freymann DM, Stroud RM, Walter P. The signal recognition particle. *Annu. Rev. Biochem.* 2001; 70:755–775. [PubMed: 11395422]
- Doudna JA, Batey RT. Structural insights into the signal recognition particle. *Annu. Rev. Biochem.* 2004; 73:539–557. [PubMed: 15189152]
- Walter P, Johnson AE. Signal sequence recognition and protein targeting to the endoplasmic reticulum membrane. *Annu. Rev. Cell Biol.* 1994; 10:87–119. [PubMed: 7888184]
- Powers T, Walter P. Reciprocal stimulation of GTP hydrolysis by two directly interacting GTPases. *Science.* 1995; 269:1422–1424. [PubMed: 7660124]
- Peluso P, Shan S.-o. Nock S, Herschlag D, Walter P. Role of SRP RNA in the GTPase cycles of Ffh and FtsY. *Biochemistry.* 2001; 40:15224–15233. [PubMed: 11735405]
- Peluso P, Herschlag D, Nock S, Freymann DM, Johnson AE, Walter P. Role of 4.5 S RNA in assembly of the bacterial signal recognition particle with its receptor. *Science.* 2000; 288:1640–1643. [PubMed: 10834842]
- Zopf D, Bernstein HD, Johnson AE, Walter P. The methionine-rich domain of the 54 kd protein subunit of the signal recognition particle contains an RNA binding site and can be crosslinked to a signal sequence. *EMBO J.* 1990; 9:4511–4517. [PubMed: 1702385]
- Keenan RJ, Freymann DM, Walter P, Stroud RM. Crystal structure of the signal sequence binding subunit of the signal recognition particle. *Cell.* 1998; 94:181–191. [PubMed: 9695947]
- Buskiewicz I, Peske F, Wieden HJ, Gryczynski I, Rodnina MV, Wintermeyer W. Conformations of the signal recognition particle protein Ffh from *Escherichia coli* as determined by FRET. *J. Mol. Biol.* 2005; 351:417–4130. [PubMed: 16005894]
- Spanggord RJ, Siu F, Ke A, Doudna JA. RNA-mediated interaction between the peptide-binding and GTPase domains of the signal recognition particle. *Nature Struct. Mol. Biol.* 2005; 12:1116–1122. [PubMed: 16299512]
- Shepotinovskaya IV, Freymann DM. Conformational change of the N-domain on formation of the complex between the GTPase domains of *Thermus aquaticus* Ffh and FtsY. *Biochim. Biophys. Acta.* 2002; 1597:107–114. [PubMed: 12009409]
- Shepotinovskaya IV, Focia PJ, Freymann DM. Crystallization of the GMPPCP complex of the NG domains of *T. aquaticus* Ffh and FtsY. *Acta Crystallog. sect. D.* 2003; 59:1834–1837.
- Focia PJ, Shepotinovskaya IV, Seidler JA, Freymann DM. Heterodimeric GTPase core of the SRP targeting complex. *Science.* 2004; 303:373–377. [PubMed: 14726591]
- Egea PF, Shan SO, Napetschnig J, Savage DF, Walter P, Stroud RM. Substrate twinning activates the signal recognition particle and its receptor. *Nature.* 2004; 427:215–221. [PubMed: 14724630]
- Shan SO, Stroud RM, Walter P. Mechanism of association and reciprocal activation of two GTPases. *PLoS Biol.* 2004; 2:e320. [PubMed: 15383838]
- Song W, Raden D, Mandon EC, Gilmore R. Role of Sec61alpha in the regulated transfer of the ribosome-nascent chain complex from the signal recognition particle to the translocation channel. *Cell.* 2000; 100:333–343. [PubMed: 10676815]
- Ahmadian MR, Mittal R, Hall A, Wittinghofer A. Aluminum fluoride associates with the small guanine nucleotide binding proteins. *FEBS Letters.* 1997; 408:315–318. [PubMed: 9188784]

18. Scheffzek K, Ahmadian MR, Kabsch W, Wiesmuller L, Lautwein A, Schmitz F, Wittinghofer A. The Ras-RasGAP complex: structural basis for GTPase activation and its loss in oncogenic Ras mutants. *Science*. 1997; 277:333–338. [PubMed: 9219684]
19. Tesmer JJ, Berman DM, Gilman AG, Sprang SR. Structure of RGS4 bound to AIF4-activated G( $\alpha$ ): stabilization of the transition state for GTP hydrolysis. *Cell*. 1997; 89:251–261. [PubMed: 9108480]
20. Rittinger K, Walker PA, Eccleston JF, Smerdon SJ, Gamblin SJ. Structure at 1.65 Å of RhoA and its GTPase-activating protein in complex with a transition-state analogue. *Nature*. 1997; 389:758–762. [PubMed: 9338791]
21. Graham DL, Eccleston JF, Chung CW, Lowe PN. Magnesium fluoride-dependent binding of small G proteins to their GTPase-activating proteins. *Biochemistry*. 1999; 38:14981–14987. [PubMed: 10555980]
22. Schlichting I, Reinstein J. pH influences fluoride coordination number of the AIF<sub>x</sub> phosphoryl transfer transition state analog. *Nature Struct. Biol.* 1999; 6:721–723. [PubMed: 10426946]
23. Sondek J, Lambright DG, Noel JP, Hamm HE, Sigler PB. GTPase mechanism of Gproteins from the 1.7-Å crystal structure of transducin  $\alpha$ -GDP-AIF-4. *Nature*. 1994; 372:276–279. [PubMed: 7969474]
24. Schindelin H, Kisker C, Schlessman JL, Howard JB, Rees DC. Structure of ADP  $\times$  AIF4(-)-stabilized nitrogenase complex and its implications for signal transduction. *Nature*. 1997; 387:370–376. [PubMed: 9163420]
25. Wittinghofer A. Signaling mechanistics: aluminum fluoride for molecule of the year. *Curr. Biol.* 1997; 7:R682–R685. [PubMed: 9382787]
26. Thomas CJ, Du X, Li P, Wang Y, Ross EM, Sprang SR. Uncoupling conformational change from GTP hydrolysis in a heterotrimeric G protein  $\alpha$ -subunit. *Proc. Natl Acad. Sci. USA*. 2004; 101:7560–7565. [PubMed: 15128951]
27. Prive GG, Milburn MV, Tong L, de Vos AM, Yamaizumi Z, Nishimura S, Kim SH. X-ray crystal structures of transforming p21 ras mutants suggest a transition-state stabilization mechanism for GTP hydrolysis. *Proc. Natl Acad. Sci. USA*. 1992; 89:3649–3653. [PubMed: 1565661]
28. Freymann DM, Keenan RJ, Stroud RM, Walter P. Structure of the conserved GTPase domain of the signal recognition particle. *Nature*. 1997; 385:361–364. [PubMed: 9002524]
29. Bernstein HD, Poritz MA, Strub K, Hoben PJ, Brenner S, Walter P. Model for signal sequence recognition from amino-acid sequence of 54K subunit of signal recognition particle. *Nature*. 1989; 340:482–486. [PubMed: 2502718]
30. Aittaleb M, Rashid R, Chen Q, Palmer JR, Daniels CJ, Li H. Structure and function of archaeal box C/D sRNP core proteins. *Nature Struct. Biol.* 2003; 10:256–263. [PubMed: 12598892]
31. Endrizzi JA, Kim H, Anderson PM, Baldwin EP. Crystal structure of *Escherichia coli* cytidine triphosphate synthetase, a nucleotide-regulated glutamine amidotransferase/ATP-dependent amidoligase fusion protein and homologue of anticancer and antiparasitic drug targets. *Biochemistry*. 2004; 43:6447–6463. [PubMed: 15157079]
32. Eads JC, Scapin G, Xu Y, Grubmeyer C, Sacchettini JC. The crystal structure of human hypoxanthine-guanine phosphoribosyltransferase with bound GMP. *Cell*. 1994; 78:325–334. [PubMed: 8044844]
33. Ollis DL, Brick P, Hamlin R, Xuong NG, Steitz TA. Structure of large fragment of *Escherichia coli* DNA polymerase I complexed with dTMP. *Nature*. 1985; 313:762–766. [PubMed: 3883192]
34. Beese LS, Derbyshire V, Steitz TA. Structure of DNA polymerase I Klenow fragment bound to duplex DNA. *Science*. 1993; 260:352–355. [PubMed: 8469987]
35. Aldaz H, Rice LM, Stearns T, Agard DA. Insights into microtubule nucleation from the crystal structure of human  $\gamma$ -tubulin. *Nature*. 2005; 435:523–527. [PubMed: 15917813]
36. Oubridge C, Ito N, Evans PR, Teo CH, Nagai K. Crystal structure at 1.92 Å resolution of the RNA-binding domain of the U1A spliceosomal protein complexed with an RNA hairpin. *Nature*. 1994; 372:432–438. [PubMed: 7984237]
37. Scapin G, Grubmeyer C, Sacchettini JC. Crystal structure of orotate phosphoribosyltransferase. *Biochemistry*. 1994; 33:1287–1294. [PubMed: 8312245]

38. Rould MA, Perona JJ, Steitz TA. Structural basis of anticodon loop recognition by glutamyl-tRNA synthetase. *Nature*. 1991; 352:213–218. [PubMed: 1857417]
39. Brautigam CA, Steitz TA. Structural principles for the inhibition of the 3'–5' exonuclease activity of *Escherichia coli* DNA polymerase I by phosphorothioates. *J. Mol. Biol.* 1998; 277:363–377. [PubMed: 9514742]
40. Silva M, Silva CH, Iulek J, Thiemann OH. Three-dimensional structure of human adenine phosphoribosyltransferase and its relation to DHA-urolithiasis. *Biochemistry*. 2004; 43:7663–7671. [PubMed: 15196008]
41. Sinha SC, Smith JL. The PRT protein family. *Curr. Opin. Struct. Biol.* 2001; 11:733–739. [PubMed: 11751055]
42. Sprang SR. G protein mechanisms: insights from structural analysis. *Annu. Rev. Biochem.* 1997; 66:639–678. [PubMed: 9242920]
43. Vetter IR, Wittinghofer A. The guanine nucleotide-binding switch in three dimensions. *Science*. 2001; 294:1299–1304. [PubMed: 11701921]
44. Poritz MA, Strub K, Walter P. Human SRP RNA and *E. coli* 4.5 S RNA contain a highly homologous structural domain. *Cell*. 1988; 55:4–6. [PubMed: 2458843]
45. Miller JD, Bernstein HD, Walter P. Interaction of *E. coli* Ffh/4.5S ribonucleoprotein and FtsY mimics that of mammalian signal recognition particle and its receptor. *Nature*. 1994; 367:657–659. [PubMed: 8107852]
46. Schmitz U, James TL, Lukavsky P, Walter P. Structure of the most conserved internal loop in SRP RNA. *Nature Struct. Biol.* 1999; 6:634–638. [PubMed: 10404218]
47. Batey RT, Rambo RP, Lucast L, Rha B, Doudna JA. Crystal structure of the ribonucleoprotein core of the signal recognition particle. *Science*. 2000; 287:1232–1239. [PubMed: 10678824]
48. Weichenrieder O, Wild K, Strub K, Cusack S. Structure and assembly of the Alu domain of the mammalian signal recognition particle. *Nature*. 2000; 408:167–173. [PubMed: 11089964]
49. Banerjee A, Yang W, Karplus M, Verdine GL. Structure of a repair enzyme interrogating undamaged DNA elucidates recognition of damaged DNA. *Nature*. 2005; 434:612–618. [PubMed: 15800616]
50. Fromme JC, Banerjee A, Huang SJ, Verdine GL. Structural basis for removal of adenine mispaired with 8-oxoguanine by MutY adenine DNA glycosylase. *Nature*. 2004; 427:652–656. [PubMed: 14961129]
51. Scheffzek K, Ahmadian MR, Wittinghofer A. GTPase-activating proteins: helping hands to complement an active site. *Trends Biochem. Sci.* 1998; 23:257–262. [PubMed: 9697416]
52. Leslie AGW. Recent changes to the MOSFLM package for processing film and image plate data. *Joint CCP4+ ESF-EAMCB Newsletter Protein Crystallog.* 1992; 26
53. Collaborative Computational Project Number 4. The CCP4 suite: programs for protein crystallography. *Acta Crystallog. sect. D.* 1994; 50:760–763.
54. Storoni LC, McCoy AJ, Read RJ. Likelihood-enhanced fast rotation functions. *Acta Crystallog. sect. D.* 2004; 60:432–438.
55. Murshudov GN, Vagin AA, Lebedev A, Wilson KS, Dodson EJ. Efficient anisotropic refinement of macromolecular structures using FFT. *Acta Crystallog. sect. D.* 1999; 55:247–255.
56. Perrakis A, Sixma TK, Wilson KS, Lamzin VS. wARP: improvement and extension of crystallographic phases by weighted averaging of multiple-refined dummy atomic models. *Acta Crystallog. sect. D.* 1997; 53:448–455.
57. Jones TA, Zou JY, Cowan SW, Kjeldgaard M. Improved methods for building protein models in electron density maps and the location of errors in these models. *Acta Crystallog. sect. A.* 1991; 47:110–119.
58. Ramirez UD, Minasov G, Focia PJ, Stroud RM, Walter P, Kuhn P, Freymann DM. Structural basis for mobility in the 1.1 Å crystal structure of the NG domain of *Thermus aquaticus* Ffh. *J. Mol. Biol.* 2002; 320:783–799. [PubMed: 12095255]
59. Kleywegt GJ, Jones TA. Detecting folding motifs and similarities in protein structures. *Methods Enzymol.* 1997; 277:525–545. [PubMed: 18488323]

60. Zwieb C, Samuelsson T. SRPDB (signal recognition particle database). *Nucl. Acids Res.* 2000; 28:171–172. [PubMed: 10592215]

\$watermark-text

\$watermark-text

\$watermark-text

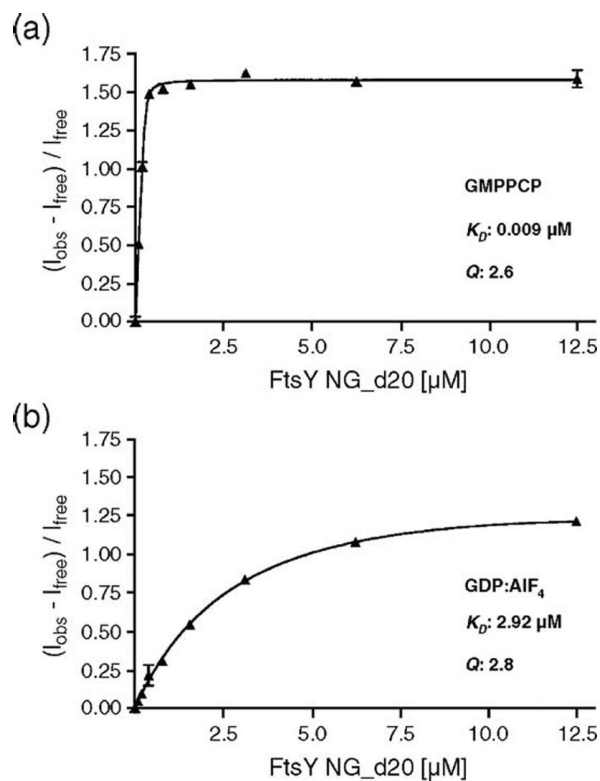


**Figure 1.**

Fluorometric measurement of binding affinity for assembly of the heterodimeric complex. (a) FRET binding data for assembly of the Ffh:FtsY NG domain heterodimer in the presence of saturating (500  $\mu\text{M}$ ) GMPPCP. The data are fit with two parameters,  $K_D$  and  $Q$  (the ratio of  $I_{\text{bound}}/I_{\text{free}}$ ), yielding a  $K_D$  of  $\sim 9$  nM. (b) Binding data for assembly in the presence of 500  $\mu\text{M}$  GDP, 0.5 mM  $\text{AlNO}_3$  and 20 mM NaF. The data are well fit with a  $K_D$  of  $\sim 3$   $\mu\text{M}$ . Note that the  $Q$  values in the two experiments are similar, as expected for assembly of the same heterodimeric complex. In each experiment, the probe species (IAEDANS-labeled Ffh E235C) was at a concentration of 0.5  $\mu\text{M}$ , and the titration was carried out over a range of 0–100  $\mu\text{M}$  FtsY\_NGd20.

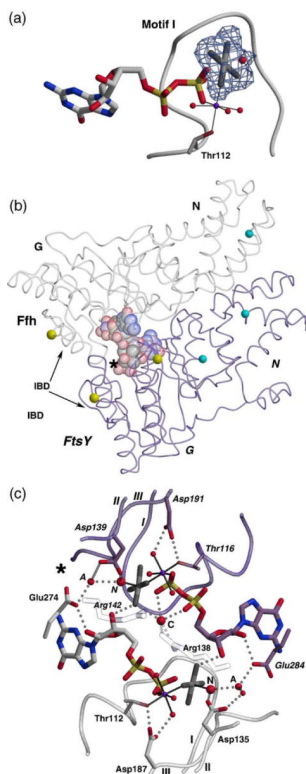


**Figure 2.**

Mg:GDP:AlF<sub>4</sub> binding within the active site chamber of the complex. (a) An omit  $F_o-F_c$  electron density map for the AlF<sub>4</sub> group and nucleophilic water molecule in the Ffh active center is shown, contoured at  $3\sigma$ , along with the GDP, coordinated Mg<sup>2+</sup> and the motif I P-loop. The square planar electron density is well defined. (b) An overview of the heterodimer structure. Ffh is shown in grey, FtsY in purple, and the domains are indicated. The location of the active site chamber is defined by the bound ligands, shown in CPK within the heterodimer backbone. The view is towards the “front” surface of the heterodimer interface.<sup>10</sup> The asterisk (\*) in all Figures indicates the location of the external nucleotide-binding site, adjacent to the FtsY active center. Colored spheres represent residues that can be located adjacent to the SRP RNA; both are discussed in the text. (c) Hydrogen bonding interactions between ligands, key active site side-chains and water molecules are shown. Hydrogen bonds are shown as dotted lines, continuous lines show the magnesium coordination and nucleophilic water molecule interactions. The magnesium ions interact with the ligands and invariant residues Thr112/116 of motif I and Asp187/191 of motif III. Invariant Asp135/139 of motif II interacts with the nucleophilic water molecules. Standard atom coloring is used for oxygen, nitrogen and phosphorus atoms, magnesium is purple. Water molecules discussed in the text are labeled: central water (C), nucleophilic water (N), auxiliary water (A). In all Figures and text, residues from FtsY are shown in italic and those from Ffh are in roman type.



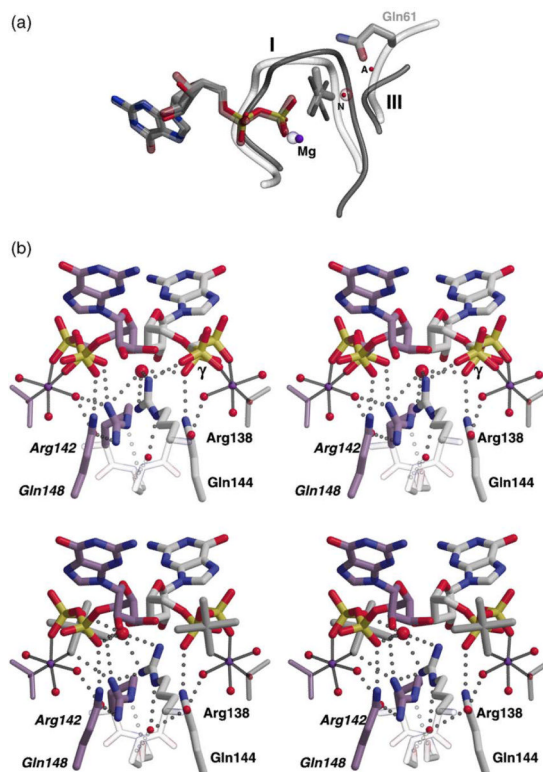


**Figure 3.**

Conformational changes in the GDP:AlF<sub>4</sub> Ffh:FtsY heterodimer. (a) The active sites of the structures of Ras: RasGAP:GDP:AlF<sub>3</sub> and Ffh:FtsY:GDP:AlF<sub>4</sub> are shown after superimposition over the nucleotide ligands. The active site of Ffh from the complex structure is shown (motif I residues 103–111, motif III residues 189–191). The Ras:RasGAP structure and its ligands are shown in thicker rendering (residues 9–17 and 59–62), with invariant Gln61 labeled. The superimposition reveals that the configuration of the P-loop (I) relative to the nucleotide in the Ffh:FtsY heterodimer is shifted compared to its position in the Ras complex. (b) A comparison of the structures (as stereo images) of the Ffh:FtsY: Mg:GMPPCP (top) and Ffh:FtsY:Mg:GDP:AlF<sub>4</sub> (bottom) complexes, highlighting interactions of Arg138/Arg142, the buried central water molecule (larger red sphere) and Gln144/Gln148 with the active site ligands (see the text). Note the shift of the central water molecule by ~1 Å between the two structures.

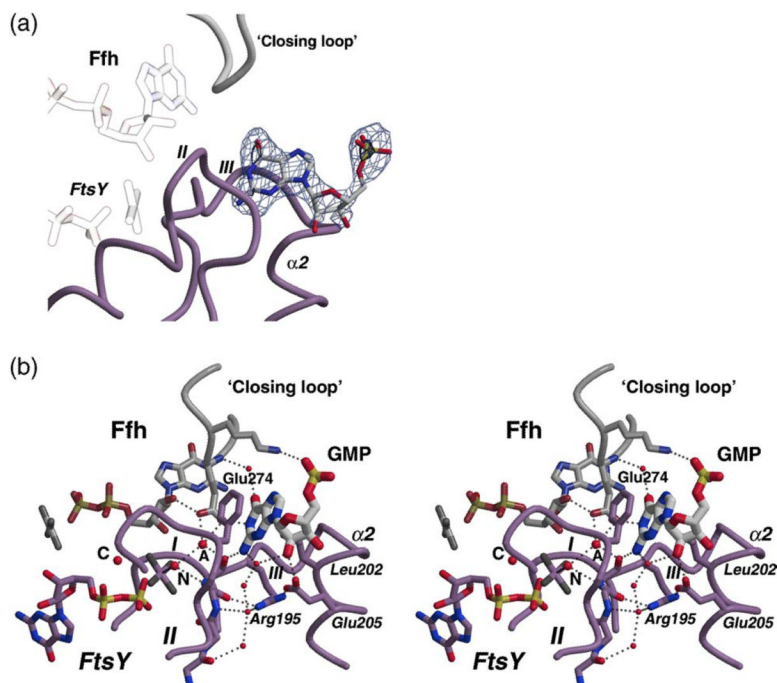


**Figure 4.**

The external nucleotide-binding site. (a) Omit  $F_o-F_c$  electron density at the external nucleotide-binding site, contoured at  $3\sigma$  (blue) and  $7.5\sigma$  (black). The density, located between motifs II and III of FtsY (below, purple) and the closing loop of Ffh (above), enters the water-filled channel that abuts the shared active site chamber,<sup>13</sup> and is close to both active site nucleotides (shown “ghosted”). (b) Stereo view of the hydrogen bonding interactions between the external GMP molecule and residues and water molecules at the complex interface are shown in an orientation similar to that in (a). Key water molecules are shown as larger spheres and labeled as in Figure 2(c). Ffh residues are highlighted in grey, FtsY residues in purple, and motifs I, II and III are labeled. *Phe141* participates in  $\pi$ - $\pi$  stacking interactions with the purine ring of the GMP molecule (front, center).

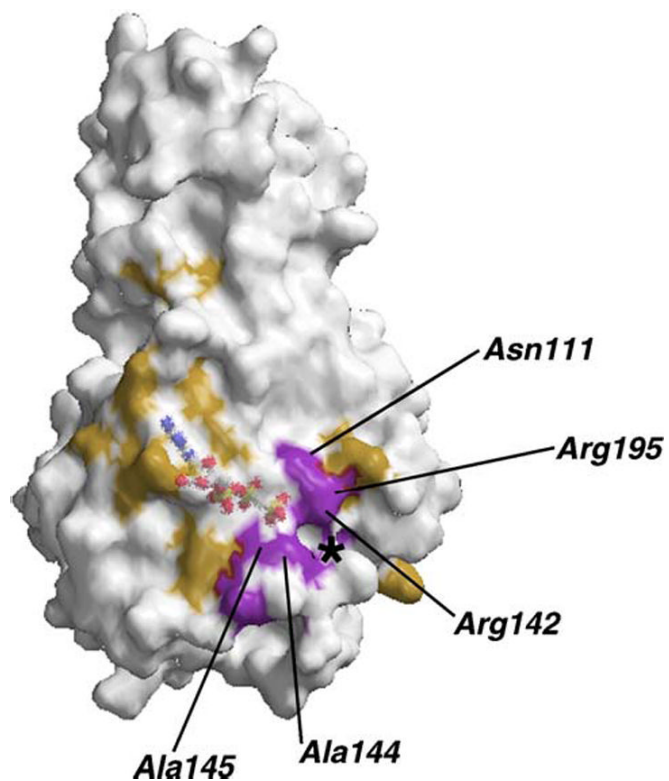


**Figure 5.** Features of the complex surface. Mutations of FtsY interface residues that affect assembly of the complex, and those that do not affect assembly but affect the subsequent GTPase hydrolysis step,<sup>15</sup> are mapped onto the surface of FtsY (gold, assembly defect; magenta, activity defect). The orientation is looking into the GTPase binding site where bound GTP is drawn as sticks. Activity defect mutations cluster (at the bottom) near the FtsY active center, locating residues that likely contribute to the activation region of the complex. The relative position of the external nucleotide site is indicated with an asterisk (\*); however, formation of that binding site requires assembly of the heterodimer.

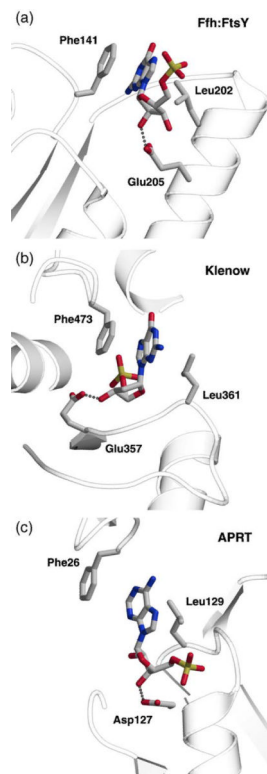


**Figure 6.**

The external site of the activation region exhibits a common nucleotide-binding structure. The phenylalanine and leucine “sandwich” interactions that position a bound nucleotide base, and a conserved acidic residue available to interact with the ribose hydroxyl, are diagrammed for a diverse set of protein families that bind nucleotides or DNA. (a) The *T. aquaticus* Ffh:FtsY:Mg:GDP: AlF<sub>4</sub>+GMP structure. (b) The 3′–5′ exonuclease site of the Klenow fragment from *E. coli* bound to single-stranded DNA (*IKFS*),<sup>39</sup> showing only the 3′-terminal nucleotide. (c) Adenine phosphoribosyltransferase from humans with bound AMP (*IORE*).<sup>40</sup>

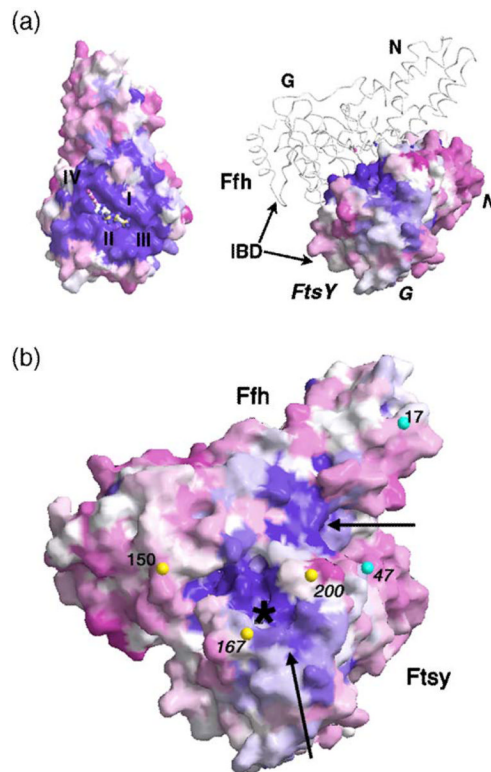


**Figure 7.**

Sequence conservation on the surface of the complex. (a) Sequence conservation in FtsY is represented as sequence entropy mapped as a gradient onto the molecular surface. Regions with high levels of sequence entropy (low conservation) are shown in pink, and regions with low levels of sequence entropy (high conservation) are shown in purple. Left: In this view of the monomer, the highly conserved GTPase sequence motifs that surround the binding pocket and that form the heterodimer interface interactions stand out. Note the triangular feature extending above and to the right of the binding pocket that corresponds to the residues of the “latch” interface of the SRP GTPase complex.<sup>13</sup> Right: Sequence conservation mapping on FtsY shown, from a lateral perspective, towards the “front” side of the interface. The backbone of Ffh (top) is indicated by a ribbon trace. (b) Sequence conservation at the heterodimer interface of the Ffh:FtsY complex. The conservation mapping reveals two outstanding patches of highly conserved sequence (indicated by arrows); the first corresponds to the “activation region”, which is the location of the external nucleoside-binding site (\*). The second (upper right) occurs near the interface of the Ffh C terminus, and the N and G domains. Colored spheres, as in Figure 2(b), mark residues that are associated with SRP 4.5 S RNA binding;<sup>10</sup> 4.5 S RNA interacts across this surface of the assembled targeting complex.

**Table 1**

## Crystallographic statistics

<i>A. Data collection</i>	
Space group	$P3_2$
Unit cell dimensions	
$a$ (Å)	188.69
$b$ (Å)	188.69
$c$ (Å)	44.59
Resolution (Å)	14.9–2.39 (2.52–2.39)
$R_{\text{sym}}$	0.101 (0.351)
Completeness (%)	99.6 (99.9)
$I/\sigma(I)$	11.7 (3.5)
Redundancy	4.1 (3.7)
<i>B. Refinement</i>	
$R_{\text{free}}$	0.252
$R_{\text{cryst}}$	0.178
RMSD from ideal	
Bond lengths (Å)	0.012
Bond angles (deg.)	1.404
Average $B$ (Å <sup>2</sup> )	
Protein	30.00
Ligand	13.00
Active site water	16.82
Other water	32.87

Values in parentheses are for the highest resolution shell.